

Title	Uraniferous dolomite: a natural source of high groundwater uranium concentrations in northern Bavaria, Germany?
Authors	Steffanowski, Jacqueline;Banning, Andre
Publication date	2017-07-26
Original Citation	Steffanowski, J. and Banning, A. (2017) 'Uraniferous dolomite: a natural source of high groundwater uranium concentrations in northern Bavaria, Germany?', Environmental Earth Sciences, 76 (15), 508, (11 pp). doi: 10.1007/s12665-017-6848-6
Type of publication	Article (peer-reviewed)
Link to publisher's version	https://link.springer.com/article/10.1007%2Fs12665-017-6848-6 - 10.1007/s12665-017-6848-6
Rights	© Springer-Verlag GmbH Germany 2017. This is a post-peer-review, pre-copyedit version of an article published in Environmental Earth Sciences. The final authenticated version is available online at: https://doi.org/10.1007/s12665-017-6848-6
Download date	2023-05-08 01:42:22
Item downloaded from	http://hdl.handle.net/10468/12341

Uraniferous dolomite – a natural source of high groundwater uranium concentrations in northern Bavaria, Germany?

Uraniferous dolomite: a natural source of high groundwater uranium concentrations in northern Bavaria, Germany?

Jacqueline Steffanowski^a, Andre Banning^{a*}

^aRuhr-Universität Bochum, Hydrogeology Department, Universitätsstr. 150, 44801 Bochum, Germany

*Corresponding author: email: andre.banning@rub.de; Tel.: +49-(0)234-32-23298

Abstract

Naturally high uranium (U) concentrations occur in the groundwater of northern Bavaria (south-eastern Germany) although the source(s) and geochemical processes controlling its occurrence are poorly understood. An earlier study identified the weathering of uraniferous apatite as responsible for elevated groundwater U in a part of the region. This present study focuses on a uraniferous dolomite facies in the Triassic sandstone aquifer of northern Bavaria as a potential source of dissolved uranium in the regional groundwater. Hydrogeochemical and mineralogical analytical methods (INAA, ICP-OES, SEP, XRD, C/S measurements), in conjunction with existing hydro- and geochemical datasets, as well as hydrogeochemical modelling approaches indicate a strong connection between groundwater U and the dolomitic facies. Highest groundwater concentrations (max: 58.3 µg L⁻¹) occur under slightly alkaline and oxic to slightly reducing conditions. Uranium speciation is dominated by mobile U(VI), predominantly in the form of uranyl-carbonate complexes. Groundwater is undersaturated with respect to U mineral phases. In addition, high values in the dolomite extraction step (SEP) and a positive correlation of dolomite (XRD) and Ca with U (INAA) support the assumption of mobilization from the uraniferous dolomite as a potential source for elevated U concentrations, and hence one of the causes for the geogenic groundwater U problem in this region.

Keywords: Triassic, dolcrete, sequential extraction, trace elements, hydrogeochemistry, mobility

1. Introduction

Uranium (U), a heavy trace metal that has the potential for toxic impacts to humans (Schnug and Lottermoser 2013, Wrenn et al. 1985, Kurttio et al. 2002), has become an important topic in environmental health research. When consumed via drinking water, it is suspected to have a nephrotoxic potential, particularly for infants and children. Moreover, ecologic studies suggest elevated risks for some cancer types when drinking water concentrations are enhanced (Wagner et al. 2011, Radespiel-Tröger and Meyer 2013). As a result, Germany established a threshold value of $10 \mu\text{g L}^{-1}$ in its Drinking Water Ordinance. Sources of the U concentrations in groundwater can be either natural or anthropogenic. Whereas the former are represented by uraniferous rocks like acid magmatites (Welte 1962, Banning 2012), the latter can result from activities such as U mining (Fernandez et al. 1996) or phosphorus fertilization (Schnug and Lottermoser 2013).

Responsible processes for high U concentrations are the oxidation of immobile U(IV) to mobile U(VI), which is driven by, amongst other factors, the influence of agricultural nitrate (Nolan and Weber 2015, Blum et al. 2016, van Berk and Fu 2017, Banning et al. 2013). Formation of uranyl complexes (Finch and Murakami 1999), e.g., with sulphate (Dorfner 1964), iron hydroxide (O'Loughlin et al. 2003, Dickinson and Scott 2010), phosphate (Bachmaf et al. 2008, Dill 1988), carbonate (Finch and Murakami 1999) and organic material (Breger and Deul 1955, Gruner 1956), is another major control of environmental U mobility. The uranyl cation UO_2^{2+} can substitute for Ca^{2+} in mineral lattices, resulting in partly substantial U contents in Ca phosphates such as apatite (Starinsky et al. 1982, Rakovan et al. 2002), or Ca carbonates such as calcite (Sturchio et al. 1998, Kelly et al. 2003). Uranium uptake by dolomite is less well characterized. Studying carbonate phases of variable Ca/Mg ratio, Deininger (1964) found no clear preference for U hosting in either calcite or dolomite. He concluded that U content in dolomite is a function of the chemical composition of the dolomitizing solution, and that U may substitute for Ca as well as Mg in the dolomite lattice.

Parts of northern Bavaria are known for high U concentrations in groundwater. Prior studies dealt with phosphatic and carbonatic uraniferous concretions, so-called phoscretes and dolcretes (together also referred to as “active arkoses”), in the Norian aquifer sediments (“Burgsandstein”) of the area (Dill 1988, Abele et al. 1962, Welte 1962). Banning and Rude (2015) showed that the weathering of phoscretes (U-rich carbonate fluorapatite) is responsible for the occurrence of high groundwater U concentrations around the city of Nürnberg. The present study aims at unravelling the U distribution, fractionation and potential mobilization mechanisms in the dolcrete area farther to the north, between the cities of Bamberg and

Coburg (Fig. 1). Hydrochemical, geochemical and mineralogical data were combined to test the hypothesis that also in this area, elevated groundwater U concentrations are caused by interaction between groundwater and uraniferous aquifer sediment intercalations.

2. Materials and Methods

2.1 Study area

The study area is located in south eastern Germany in the federal state of Bavaria, around the city of Bamberg (Fig. 1). Geologically, it is part of the German Keuper Basin, filled with late Triassic terrestrial and shallow marine sediments. This includes one of the most important regional aquifers (the “Burgsandstein”), which is used for water extraction. According to Heinrichs and Udluft (1999), the typical groundwater quality in this approximately 120 m thick coarse sandstone unit is Ca-Mg-HCO₃. “Active arkoses”, however, exclusively appear in the upper approximately 70 m of this aquifer system (Middle and Upper “Burgsandstein”; Banning and Rude 2015).

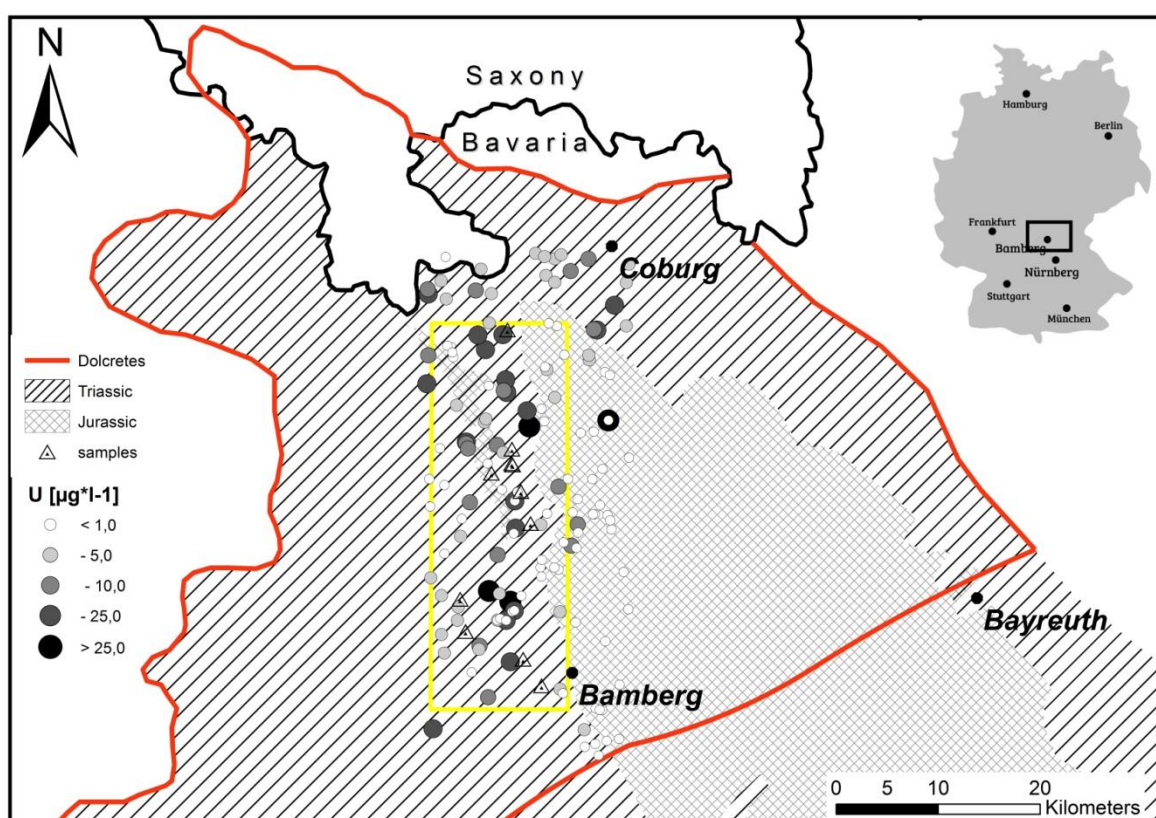


Fig. 1 Distribution of U concentrations in groundwater (circles; data kindly provided by the Bavarian Environment Agency, LFU) of the study area (yellow box), the range of the Triassic sandstone facies and rock sampling locations (triangles). The distribution of the dolcrete facies according to Dill (1988) is bordered in red.

Dill (1988) described three different U-bearing facies in the "Burgsandstein" aquifer system: (1) silcretes, (2) calcretes/dolcretes, and (3) phoscretes. The research for this present study focused on an area where calcretes/dolcretes occur (Fig. 1). This carbonatic cement syndiagenetically incorporated U, which has its origin in the alteration of the mostly granitoidic Vindelician Swell (a meanwhile eroded part of the Central European Moldanubian Variscides), during the sandstone carbonation (Welte 1962, Banning 2012).

The granitoidic character of its parental rocks gave rise to an increased amount of feldspar in the sandstone (often >25 vol.%) at the expense of quartz, conforming to the definition of an arkose. The feldspar is an indicator for short transport, a high accumulation rate and a low degree of chemical alteration (Füchtbauer 1988). Because uraniferous intercalations have incorporated radioactive elements through sorption and ionic substitution (as was detected during U exploration programmes in the 1950s), these sandstones are referred to as "active arkoses".

Similar geological observations documenting a connection between dolomite and U concentrations were made worldwide, e.g., in Somalia (Mudugh), Kyrgyzstan (Tyuya Muyun), and the USA (Pryor Mts., Colorado) (Dahlkamp 1979; Nash 1979; Briot 1983). In these cases, U was concentrated in duricrusts composed of cement-forming calcite (calcretes), gypsum (gypcretes), dolomite (dolcretes), halite (salcretes), and ferric oxide (ferricretes) (e.g., Dill 2009 and references therein).

Based on information given by the weather station Bamberg (+240 m a.s.l.) recording both temperature and precipitation, the region has an average temperature from 0.3 °C (January) up to 19.0 °C (July). The measured absolute maximum temperatures vary from 14.5 °C (January) to 37.8 °C (August) and the absolute minimum temperatures from -20.9 °C (January) to 8.1 °C (June). These are average values of the last decade (04/2007 – 04/2017) and were updated monthly. Average precipitation during the same period was determined as 32 mm (February) up to 75 mm (July). Annual average temperature is about 9.4 °C, annual precipitation about 650 mm on average.

2.2 Available hydrochemical and geochemical data

Several datasets on the study area were kindly provided by the *Bavarian Environment Agency (LfU)* and include geological, geochemical, as well as hydrochemical information from the "Burgsandstein" and other regional aquifers. Because this study focused on uranium, only the hydrochemical datasets in which U was analyzed were used. This yielded 114 sets of data (54 groundwater samples and 60 spring water samples), which were collected between 1971 and

2014. It also contains information on major and minor ion concentrations as well as physico-chemical parameters. Figure 1 depicts the occurrence of U in groundwater during the mentioned time period; and, because Bavaria's water supply system is highly decentralized, it also represents the drinking water quality. Concentrations of redox-sensitive parameters were used to assign a general redox status to each sample following to the procedure described by Jurgens et al. (2009).

2.3 Rock sampling and analytical procedures

A total of 15 rock samples from 11 locations were collected from outcrops of the Upper and Middle “Burgsandstein” (Fig. 1). These were taken according to an optical differentiation between “normal” aquifer sandstones serving as reference samples (n=7), and carbonatic intercalations within the sandstone (n=8). All samples were analysed for bulk rock geochemistry (49 elements) using Instrumental Neutron Activation Analysis (INAA, thermal neutron flux: $7 \times 10^{12} \text{ n cm}^{-2} \text{ s}^{-1}$, Ge detector: resolution better than 1.7 keV for the 1332 keV, ^{60}Co photopeak) and total digestion ($\text{HClO}_4\text{--HNO}_3\text{--HCl--HF}$ at 240 °C) followed by ICP-OES analysis. These analyses were performed by Activation Laboratories Ltd., Ancaster, Ontario/Canada. Analytical quality was ensured by duplicate and blank measurements, and usage of certified reference materials such as GXR-1, 4 and 6; DNC-1a; SBC-1; OREAS 45d; SdAR-M2 and DMMAS 119 (the latter used for U determination).

Based on the geochemical results as well as the macroscopic rock identification, 10 samples were selected for XRD analyses to characterise their mineralogical composition, with special attention given to both the dolomite component and U contents. The samples were ground to powder grain size in a tungsten carbide mill before measurements were performed on a PANalytical Diffractometer Empyrean (PANalytical B.V., Almelo, Netherlands) with a vertical Theta-Theta Goniometer including Bragg-Brentano-Geometry (operational adjustments: 40 kV, 45 mA; 2θ range: 4.0-65.0°, step size: 0.01° 2θ , anode material: Cu). Two samples (Dol_6, Dol_7) were measured a second time after passing the sequential extraction procedure (SEP) to study possible changes in the mineralogical composition and to evaluate the SEP's dissolution efficiency.

Five samples with U contents $>1 \mu\text{g g}^{-1}$ (range: 1.6-36.6 $\mu\text{g g}^{-1}$) and one reference aquifer sandstone sample with $\text{U} < 0.5 \mu\text{g g}^{-1}$ (and without dolomite) were subjected to a sequential extraction procedure (SEP) as described by Regenspurg et al. (2010) and Wenzel et al. (2001), slightly modified in centrifuge speed (20 min, 5000 rpm) and solid/solution ratio (SSR) (Table 1). The SSR was modified to insure that the dolomite in these samples would

completely dissolve. The successful extraction of dolomite using NaAc (1 M) in acetic acid (25 %) is reported by both Tessier et al. (1979) and Eichfeld (2004). The required SSR was calculated using equilibrium modelling with *PHREEQC 3* (Parkhurst and Appelo 2013), resulting in at least 50 ml solution for 300 mg dolomite. Because 1 g of sample was placed in a 50-ml container to perform the extraction, this step required three repetitions (except for one sample with the highest dolomite content taking four repetitions, and the dolomite-free reference sample with only one repetition). A further variation from Regenspurg et al. (2010) was to limit the repetitions of the step targeting organically bound U to 1, because both the marginal amount of organic material in the regional “active arkose” as reported by Abele et al. (1962) and our own results from C_{org} measurements (cf. 3.2).

Aliquots of the powder (1 g), which was also used in XRD measurements, were placed in 50 ml centrifugation tubes and extraction solutions were added in each step, followed by the decantation of each used solution. Every powder sample was subjected to the entire procedure (Table 1). Extracted solutions were analysed for U concentrations using ICP-MS (Agilent 7900, Santa Clara, USA; analytical detection limit: $0.1 \mu\text{g L}^{-1}$).

Table 1: Applied sequential extraction procedure, modified from Regenspurg et al. (2010) and Wenzel et al. (2001).

Step no.	Target U fraction	Extractant	Procedure	Repetition	SSR*
1	Easily mobilisable	MgCl ₂ (0.4 M)	1 h shaking	1x	1:25
2	Bound to organic matter	NaOCl (5-6 %)	1 h shaking	1x	1:25
3	Bound to carbonate	NaAc (1 M) in acetic acid (25%)	2 h shaking	**3x	**1:150
4	Bound to Fe- and Mn-Hydr(oxide)	NH ₄ -oxalate (0.2 M) with acetic acid (1 M); pH=2	5 h shaking in the dark	1x	1:25
5	Residual	Calculated with $U_{tot} - U_{\sum \text{steps } 1-4}$			

*SSR = Solid Solution Ratio, **except for two samples: highest dolomite content – 4 (1:200); dolomite-free sample – 1 (1:25)

Additionally, samples were dried and weighed to determine extraction mass loss during SEP, i.e. the difference between initial and output weight. For dolomite bearing samples, a weight loss percentage in the same range as the dolomite contents confirmed that the applied extractant is suitable for dolomitic rock samples. Further aliquots of the six samples were

analyzed for carbon (C_{org}/C_{inorg}) and sulfur (S_{total}/S_{pyrite}) contents in a combustion analyser (G4 ICARUS HF, Bruker, Billerica, MA, USA; analytical detection limit: 0.01 wt.%).

2.4 Hydrogeochemical modelling

In this study the hydrochemical groundwater dataset was used to model U speciation and the stability of potential U phases and other minerals applying the code PhreeqC 3 (Parkhurst and Appelo 2013). The databank *minteq.v4.dat* was selected for the calculations. Since the hydrochemical dataset did not include information about the current redox potential, the applied pE values were estimated using the aforementioned redox categories following the method described by Jurgens et al. (2009), and assigning pE values representative for these redox categories (Drever 1997; Huang et al. 2011).

3. Results and discussion

3.1 Uranium distribution in the aquifer

Uranium concentrations in the groundwater near Bamberg are presented according to their geologic host formation in Table 2. The spatial distribution of these values is shown in Figure 1.

Table 2: Uranium groundwater concentrations ($\mu\text{g L}^{-1}$) in various geologic formations.

Rock formation	Triassic		Triassic/Jurassic		Jurassic	Quaternary
	“Burg-sandstein”	undiff. sandstone	Rhaetian-Lower Jurassic transient layer	Rhaetian sandstone	Lower Jurassic	fluvialite deposits
	(n=61)	(n=8)	(n=13)	(n=18)	(n=4)	(n=10)
U_{Max} ($\mu\text{g L}^{-1}$)	42.33	19.77	7.066	6.677	2.773	1.906
U_{Mean} ($\mu\text{g L}^{-1}$)	7.237	7.704	1.081	1.403	1.385	0.654
U_{Min} ($\mu\text{g L}^{-1}$)	0.325	0.899	0.006	0.090	0.323	0.032

Table 2 shows that the highest dissolved uranium concentrations were measured in the “Burgsandstein”, followed by undifferentiated Triassic sandstone (which may include some samples from the “Burgsandstein”). The mean and minimum values are also highest in these formations. Younger sedimentary units (Triassic/Jurassic, Jurassic, and Quaternary) have much lower maximum and mean U concentrations, as is reflected in Figure 1.

Groundwater in the study area indicates dominantly circumneutral pH conditions (mean: 7.3, ranging from 4.4 to 9.2). A plot of U against pH reveals no correlation between these parameters. However, it shows that the highest U concentrations occur in the neutral to slightly alkaline pH milieu, whereas no threshold-exceeding concentrations are found at pH < 6.7 and > 7.7 (Fig. 2).

Based on the redox assignment obtained using the procedure described by Jurgens et al. (2009), four groundwater redox milieus were distinguished in the study area. The majority of waters is oxic, i.e. O₂-reducing (86 %), fewer waters plot in the Mn- and/or NO₃⁻- (together 8 %) and Fe(III)/SO₄²⁻- (6 %) reduction ranges. Elevated U concentrations (> 10 µg/L) occur under oxic and slightly reducing conditions (not in the Fe/SO₄-reducing milieu), as might be expected from an understanding of the geochemical controls on U mobility (cf. 1.1). However, there is no clear relationship between redox conditions and elevated U in the study area, which suggests that U is not mobilized from the aquifer matrix through oxidation, as has been found in other studies (e.g., Banning et al., 2013).

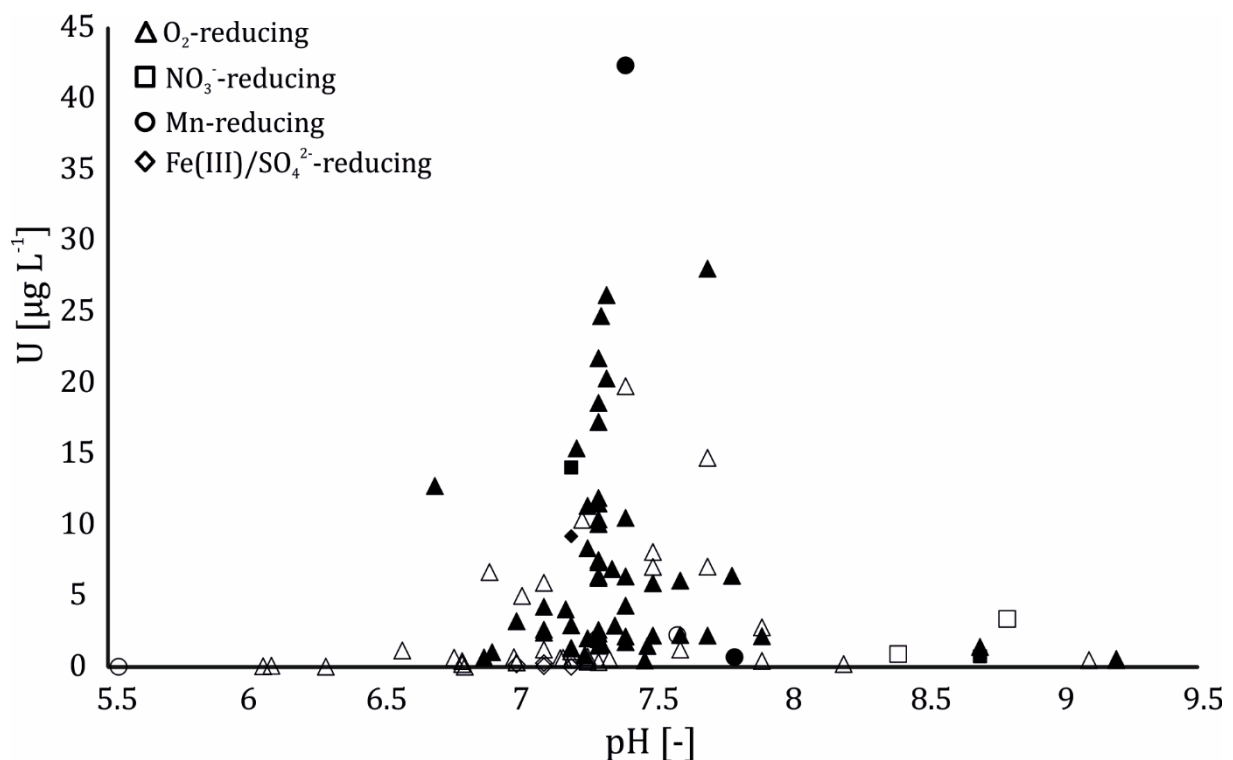


Fig. 2: pH-dependent distribution of U concentrations in groundwater within the study area. Symbols indicate redox assignments made using the methodology of Jurgens et al. (2009). Filled symbols are data from the "Burgsandstein" aquifer; hollow symbols are data from undifferentiated sandstone and other aquifers.

In terms of cations, groundwater chemistry is dominated by Ca²⁺ and Mg²⁺ in nearly equal proportions, while HCO₃⁻ is the dominant anion (Fig. 3) leading to Ca-Mg-HCO₃ as the

typical groundwater quality. This is consistent with the characterization of groundwater in the "Burgsandstein" aquifer reported by Heinrichs and Udluft (1999) and indicates that dolomite dissolution is controlling the overall water quality. Only few samples contain considerable SO_4^{2-} concentrations. These almost exclusively occur in groundwater samples from late Triassic and Jurassic sediments, hardly in the "Burgsandstein" itself. Some relatively Na^+ -rich samples from the "Burgsandstein", mainly of the Na-HCO_3 quality type, were probably generated by ion exchange processes. Sporadic elevated SO_4^{2-} or Cl^- concentrations in "Burgsandstein" groundwater samples may be explained by dissolution of evaporites such as gypsum and halite, partly occurring in Triassic sediments of the study area (Reinhardt and Ricken, 2000).

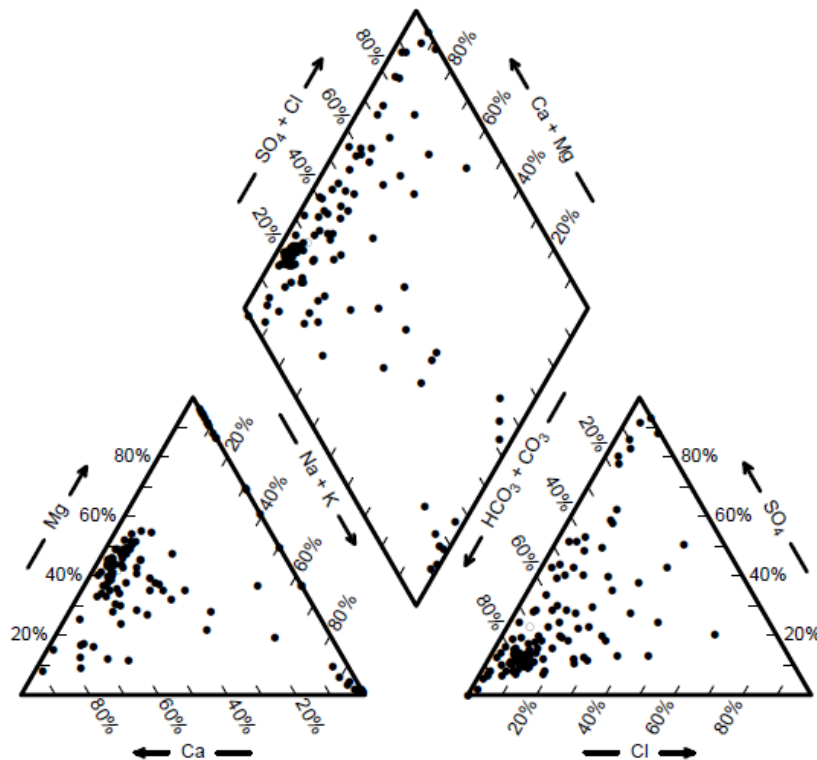


Fig. 3: Piper plot of studied groundwater samples.

3.2 Geochemistry and mineralogy

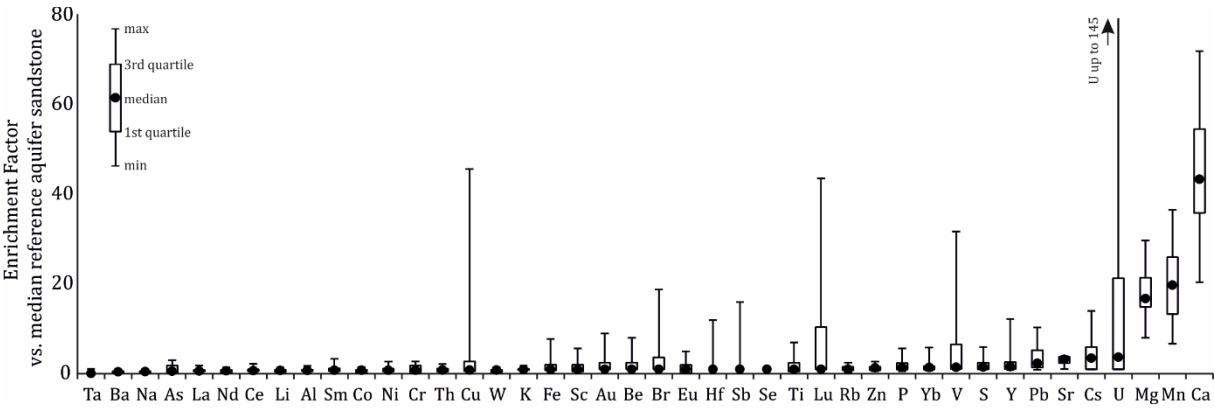
Table 3 presents the results of "Burgsandstein" rock sample analyses, which include seven "normal" (reference) sandstone samples (Ref_1 through Ref_7) and eight dolomitic sandstone samples (DoI_1 through DoI_8), as described in Section 2.2. The mean U content of the reference samples is $1.1 \mu\text{g g}^{-1}$ (ranging from <0.5 to $3.7 \mu\text{g g}^{-1}$), whereas the mean U content of the dolomitic samples is $7.1 \mu\text{g g}^{-1}$ (ranging from <0.5 to $36.3 \mu\text{g g}^{-1}$). These data support

the hypothesis that U is incorporated within the carbonatic cements of the dolomitic sandstone.

Table 3: Geochemistry (selected elements) of the “Burgsandstein” rock samples (LOD: analytical limit of detection; ICP: ICP-OES analysis following total dissolution; INAA: instrumental neutron activation analysis, cf. 2.2).

element unit method LOD	Ca (wt.%) ICP 0.01	Mg (wt.%) ICP 0.01	Al (wt.%) ICP 0.01	K (wt.%) ICP 0.01	P (wt.%) ICP 0.001	Fe (wt.%) INAA 0.01	Mn ($\mu\text{g g}^{-1}$) ICP 1	U ($\mu\text{g g}^{-1}$) INAA 0.5	As ($\mu\text{g g}^{-1}$) INAA 0.5	Pb ($\mu\text{g g}^{-1}$) ICP 3	Zn ($\mu\text{g g}^{-1}$) ICP 1
<i>Sandstones</i>											
Ref_1	0.10	0.34	3.54	1.46	0.009	0.41	139	<0.5	3.9	9	9
Ref_2	5.02	0.39	2.15	1.38	0.009	0.2	182	<0.5	5.4	9	17
Ref_3	2.26	1.34	3.08	1.65	0.011	0.37	397	<0.5	2.6	11	10
Ref_4	0.27	1.02	5.86	2.78	0.020	1.01	67	2.9	2.0	12	13
Ref_5	0.25	1.10	5.93	2.52	0.020	1.84	59	3.7	3.4	15	20
Ref_6	0.01	0.08	1.25	0.07	0.004	0.52	49	<0.5	<0.5	6	7
Ref_7	0.08	0.38	2.77	1.18	0.009	0.28	12	<0.5	1.3	6	6
<i>Dolcretes</i>											
DoL_1	12.7	7.51	1.74	1.24	0.009	0.11	1710	1.7	4.9	39	12
DoL_2	10.8	6.53	2.55	1.37	0.016	0.32	1290	<0.5	2.7	21	14
DoL_3	5.10	3.13	2.18	1.15	0.007	0.39	633	<0.5	<0.5	8	6
DoL_4	10.9	6.43	1.85	1.41	0.009	0.29	447	1.6	<0.5	11	6
DoL_5	7.35	3.97	2.73	2.04	0.020	0.39	1360	<0.5	<0.5	13	8
DoL_6	9.50	6.56	5.43	2.67	0.051	3.17	979	16.2	4.9	71	27
DoL_7	16.5	10.9	2.83	1.35	0.027	1.09	1840	36.3	7.8	93	20
DoL_8	18.0	11.6	1.89	1.12	0.005	0.74	2450	<0.5	<0.5	21	14

The bulk rock geochemistry of the uraniferous dolomitic sandstone samples was compared to that of the reference sandstone samples using Enrichment Factors (EF), which are calculated by dividing the elemental content of each dolomitic sample by the corresponding median value for the reference sandstones. The results, shown in Figure 4, reveal several differences between the two categories of rock samples. Two obvious differences are for the elements Mg (median EF = 17) and Ca (median EF = 43), which reflects the presence of dolomite in the uraniferous samples (Ca and Mg are also strongly correlated in these samples). Uranium is enriched by a factor of 3.7 (on average), but the maximum EF value of 145 reveals the heterogeneous nature of the "active arkoses". The median EF values for Mn (20), Cs (3.5), Sr (3.2), and Pb (2.3) indicate that these elements are also concentrated within the carbonatic cement. The remaining elements occur either in similar abundance or are depleted relative to the reference sandstone samples (Table 3, Fig. 4).



263

264

Fig. 4: Element enrichment/depletion of dolomitic samples compared to median reference sandstone contents.

265

266

267

268

269

270

271

272

273

274

275

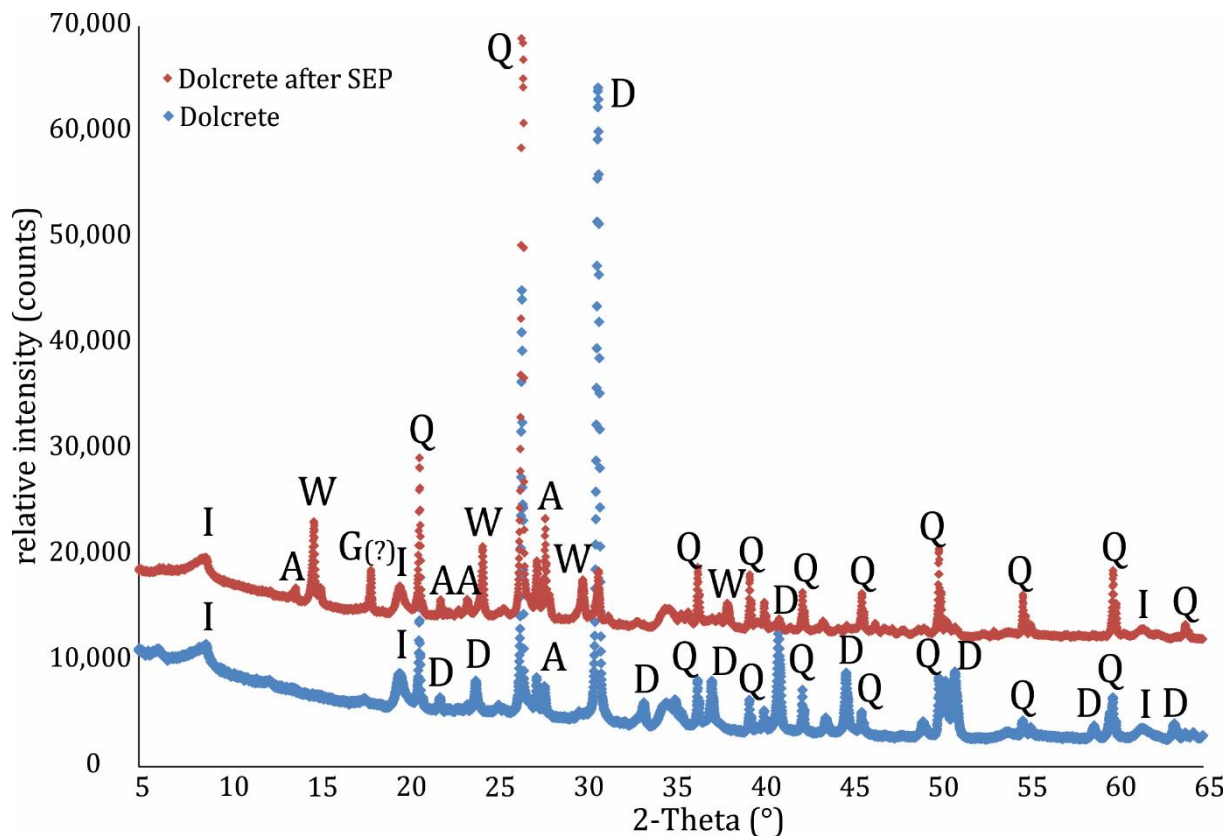
Quantitative XRD analyses indicate that the sampled reference “Burgsandstein” is dominantly composed of quartz (70-78 wt.%) and feldspar (15-25 wt.%), with minor amounts of clay minerals, calcite, and dolomite (Table 4). Increasing dolomite content in the dolcrete samples is mainly at the expense of quartz; feldspar contents remain in the order of the reference sandstones. This implies that dolcrete intercalations dominantly consist of dolomite (18-72 wt.%), feldspar (8-22 wt.%), as well as quartz (around 8-73 wt.%). Muscovite/illite, kaolinite, chlorite – together representing the clay minerals – and calcite make up the minor and accessory phases.

Table 4: Quantitative XRD results of the Triassic rock samples (n.d. – not detected).

Sample	Quartz (wt.%)	Feldspar (wt.%)	Dolomite (wt.%)	Clay minerals (wt.%)	Calcite (wt.%)
<i>Sandstones</i>					
Ref_1	70	25	n.d.	5	n.d.
Ref_2	78	15	n.d.	2	5
Ref_3	70	15	10	3	2
<i>Dolcretes</i>					
Dol_1	45	20	35	n.d.	<1
Dol_2	40	22	37	1	n.d.
Dol_3	73	8	18	1	n.d.
Dol_4	41	21	38	<1	n.d.
Dol_5	51	19	25	5	n.d.
Dol_6	20	18	45	17	n.d.
Dol_7	8	10	72	10	n.d.
<i>Dolcretes after SEP</i>					
Dol_6_SEP	58	29	3	10	n.d.
Dol_7_SEP	29	31	25	15	n.d.

276

277 Two samples were analyzed by XRD a second time after the SEP (cf. 3.3) and exhibited two
278 new mineral phases: whewellite ($\text{Ca}(\text{C}_2\text{O}_4 \cdot \text{H}_2\text{O})$) and (probably) gibbsite ($\text{Al}(\text{OH})_3$), neither of
279 which was present in the first round of XRD analyzes (Fig. 5). Because these new mineral
280 phases appeared in both samples, it is likely that they formed as a result of sample reaction
281 with one of the extraction solutions.



282

283 Fig. 5: Comparison of the XRD analysis of dolcrete sample Dol_6 before (blue) and after (red) the sequential extraction
284 procedure. Different peak positions and heights display changes in mineralogical composition (D: dolomite, Q:
285 quartz, I: illite/muscovite, W: whewellite, G: gibbsite, A: albite).

286

287 The occurrence of whewellite might be traced back to botanical relics incorporated in the bulk
288 rock samples, which have been dissolved by one of the solutions during the SEP. Nakata
289 (2003) reported that many plants contain calcium oxalate phytolites in their leaves, bark and
290 wood as monoclinic whewellite crystals. A second, and in this case more likely scenario, is
291 described by Maia et al. (2012), who treated samples containing gypsum and epsomite with a
292 mixture of ammonium oxalate and oxalic acid (similar to SEP step 4 in this study, Table 1),
293 also resulting in the precipitation of whewellite. Adapted to the present study, gypsum might
294 have temporarily been formed due to one of the first three extraction steps (Cappuyens et al.

2007), leading to precipitation of whewellite after the fourth step. Also in connection with the marginal amount of organic matter in the studied samples (Table 5), whewellite precipitation here is more likely caused by the ammonium oxalate step, as described by Maia et al. (2012). Results furthermore show that the majority of the dolomite in these samples (65 and 93 % of the initial dolomite content) – but not all of it – was dissolved during the SEP. Accordingly, quartz and feldspars became relatively enriched.

As mentioned previously, all rock samples contain minor amounts of organic matter (Table 5), which is consistent with the study conducted by Abele et al. (1962). The greatest percentage of carbon in dolcretes is inorganic (5-10 wt.%), as would be expected for samples containing dolomite. S_{pyrite} as well as S_{total} values are negligible.

Table 5: Results of carbon/sulphur measurements.

Sample	S_{pyrite} [wt.%]	S_{total} [wt.%]	C_{inorg} [wt.%]	C_{org} [wt.%]
Ref_1	< 0.01	< 0.01	0.02	0.04
Ref_4	< 0.01	0.02	0.07	0.03
Dol_1	< 0.01	0.04	6.40	0.13
Dol_4	< 0.01	0.02	6.35	0.10
Dol_6	< 0.01	0.02	5.25	0.75
Dol_7	< 0.01	0.04	9.65	0.15

Consistent with results reported by Welte (1962), Ca content (INAA) plotted against dolomite content (quantitative XRD) shows a positive correlation ($R^2 = 0.85$, $p < 0.05$) for the samples analyzed in this study (Fig. 6). Elevated U contents (> 0.5 ppm) occurred in samples where the Ca content exceeded 10 wt.% and the dolomite content exceeded 30 wt.%. This supports the conclusions of Welte (1962) and of Abele et al. (1962), who also reported that dolomite is enriched in U, possibly due to the exchange of U for Ca or Mg in the crystal lattice.

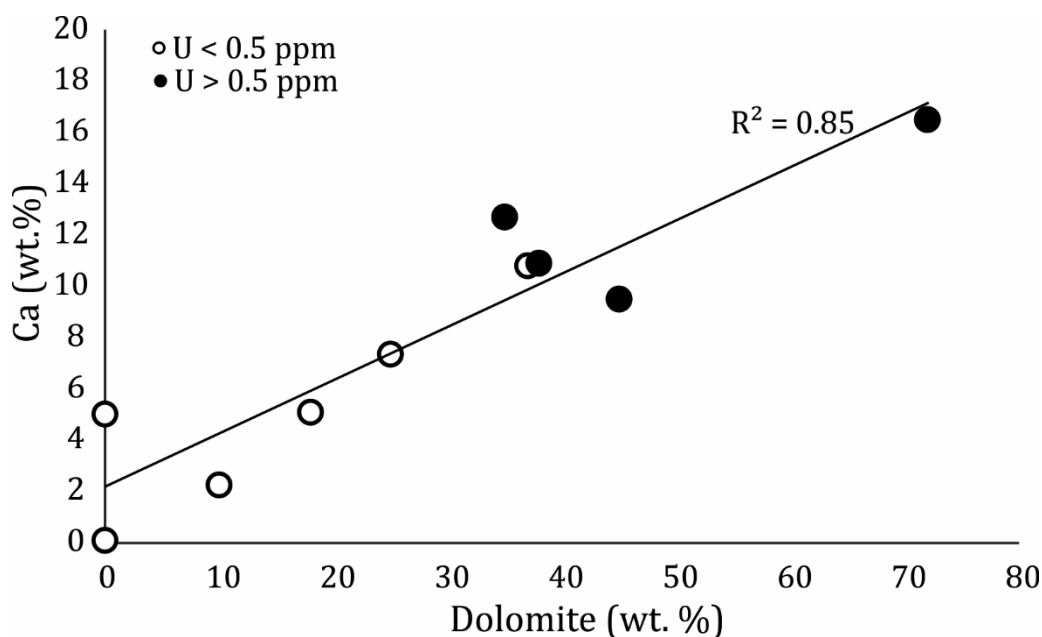


Fig. 6: Correlation of quantitative dolomite (XRD, wt.%) and Ca (INAA, wt.%) with U contents (INAA).

3.3 Uranium fractionation, remobilisation and speciation

The sequential extraction procedure (SEP) enables an assessment of U mineralogical fractionation and remobilisation behaviour. Results show that U rarely occurs in the easily mobilisable fraction (SEP step 1, Fig. 7). The U bound to organic matter (step 2) is also a very minor percentage of the total content. Apart from the residual fraction, most U is bound to carbonate/dolomite (step 3), with a maximum value of $14.6 \mu\text{g g}^{-1}$, corresponding to 41 % U_{tot} in the sample containing the highest dolomite content. Concentrations measured by the amorphous Fe hydroxide targeting step (step 4) reached a maximum value of $10.5 \mu\text{g g}^{-1}$, corresponding to 29 % U_{tot} in the sample with highest Fe (3.17 wt.%). The mass of sample dissolved during the SEP (in % initial weight) was determined by weighing prior to and after the procedure, yielding values between 5 and 50 %. Together with quantitative XRD results (Table 4), this implies that the residual fraction could indeed be lower than shown in Figure 7 and that the dolomite-bound U content could be higher, because not all dolomite was dissolved in the SEP step. In any case, high-dolomite samples were most likely to release high concentrations of U (70 % of the U_{tot} was dissolved in the SEP procedure). In contrast, reference sandstone samples subjected to SEP show considerably lower mobilization potentials, with residual fractions >80 % U_{tot} , and much lower absolute U contents. Here, minor fractions (<10 % U_{tot} each) are bound to organic matter and Fe hydroxides (Fig. 7).

Another important parameter may be rock weathering, which can have an effect on U contents and fractionation. A similar study of geogenic U behavior documented a decreasing trend in U contents with the degree of rock weathering, indicating the release of U to groundwater during rock alteration (Banning and Rde 2015). However, all samples analysed in this study were taken from comparably fresh outcrop surfaces and therefore assumed to have experienced similar degrees of weathering. Differences in weathering phenomena were not observed.

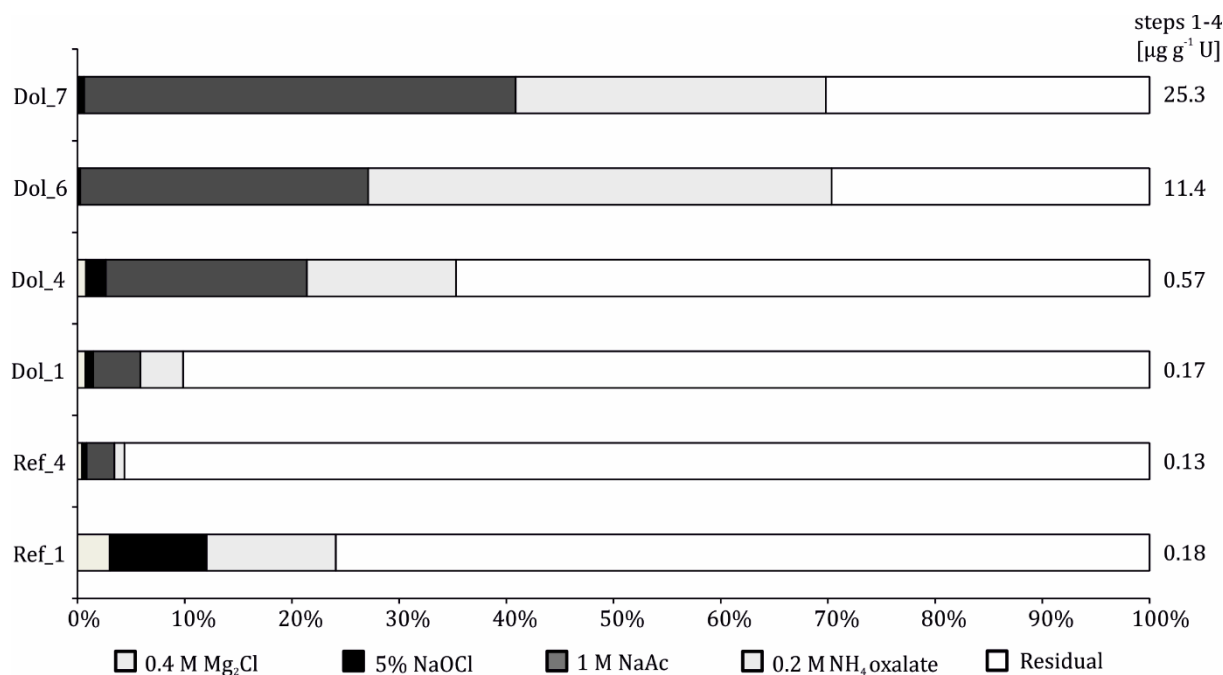


Fig. 7: Results of the sequential extraction procedure.

Furthermore, a positive (however statistically insignificant, $p > 0.05$) correlation ($R^2 = 0.73$) between the quantitative dolomite content and the determined dolomite-hosted (NaAc-soluble) U concentrations was observed (Fig. 8). Increasing dolomite content appears to implicate a higher potential for U release.

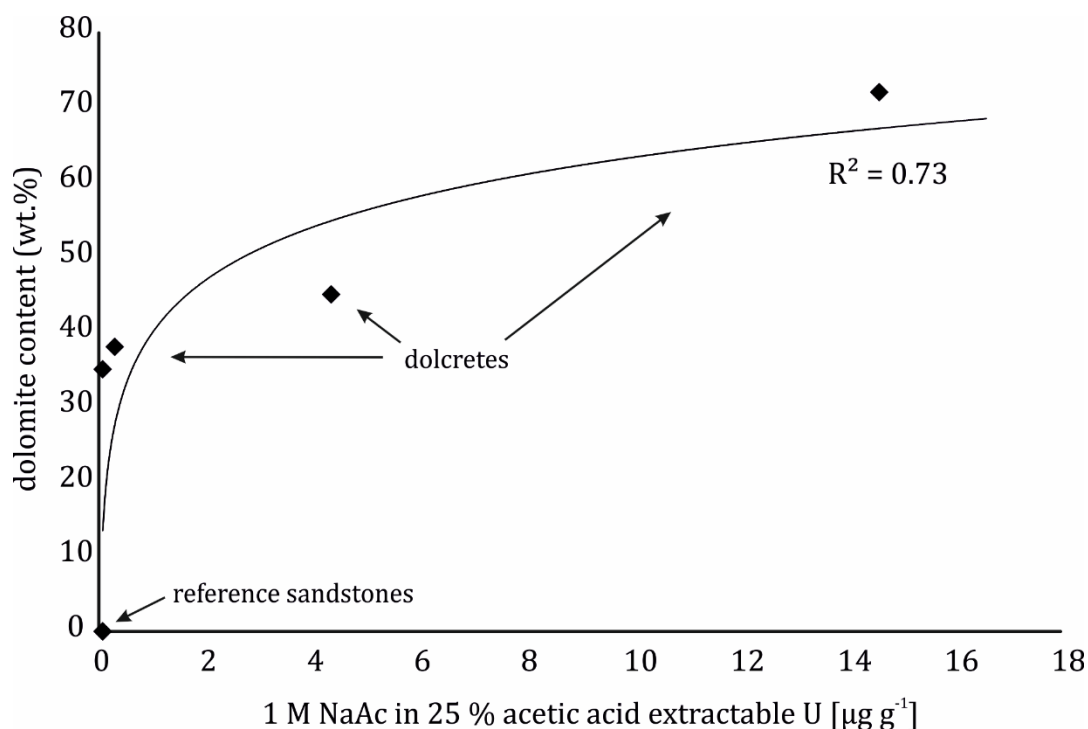


Fig. 8: Content of dolomite-bound U (extracted with 1 M NaAc in 25 % acetic acid) vs. dolomite content (XRD).

In aqueous systems, U concentrations and mobility are mainly controlled by pH, redox conditions, and the available species that can serve as complexing agents (Langmuir 1997). Under the prevailing pH and redox conditions found in the "Burgsandstein" aquifer, speciation modeling indicates that dissolved U occurs mostly in the form of uranyl-carbonate complexes (such as UO_2CO_3 , $\text{UO}_2(\text{CO}_3)_2^{2-}$, and $\text{UO}_2(\text{CO}_3)_3^{4-}$), followed by (in descending order) complexes formed with sulfate, nitrate, and hydroxide ions. Complexation with phosphates, vanadates, silicates, and other species is not significant.

Geochemical modeling also revealed that groundwater in the study area is largely undersaturated with respect to dolomite. This indicates that dolomite dissolution is possible, which could release additional dolomite-bound U to groundwater. Uraninite and other mineral phases with stoichiometric U are also undersaturated (with SI values between -28.5 and -1.5). Precipitation is therefore an unlikely mechanism for the removal of geogenic U from groundwater under current hydrogeochemical conditions.

4. Conclusions

Parts of the "Burgsandstein" aquifer system in northern Bavaria are comprised of a dolomitic sandstone facies ("dolcrete") that produces a Ca-Mg-HCO₃ type of groundwater quality. Samples of this sandstone analyzed for mineralogy and subjected to a sequential extraction

procedure revealed that uraniferous intercalations have a significant potential to release U to groundwater and are susceptible to dissolution. Geochemical modeling suggests that the prevailing pH and redox conditions favor the occurrence of U in its mobile, U(VI) oxidation state, which forms stable uranyl-carbonate complexes. Thus, these uraniferous dolcretes, along with their apatitic equivalents located farther to the south ("phoscretes", characterized in an earlier study), are important controls on the occurrence of geogenic U in a region of Germany where geogenic U contamination is most pronounced.

Apart from its regional significance, this study underscores the importance of characterizing both the aquifer matrix and the groundwater geochemistry in order to fully understand the occurrence of geogenic contaminants. In the case of a trace element whose mobility is controlled by numerous factors that can vary spatially over even small distances, a thorough understanding of the local and regional environment is crucial. This is particularly true for geogenic U, an "emerging" contaminant that is now receiving increased attention worldwide in environmental and health-related studies.

Acknowledgements

The Bavarian Environment Agency (LfU) is acknowledged for providing hydrochemical and geochemical data. The authors thank Dr. Thomas Reinecke, Mr. Oliver Schübbe and Mr. Frank Hansen (all Ruhr-Universität Bochum) for assistance in experimental and analytical work, and M.Sc. Alexander Potrafke (Universität Innsbruck) for support during rock sampling in the field, and for discussions.

References

- Abele G, Berger K, Salger M (1962) Die Uranvorkommen im Bursandstein Mittelfrankens. *Geologica Bavarica* 49:3-90.
- Bachmaf S, Planer-Friedrich B, Merkel BJ (2008) Effect of sulfate, carbonate, and phosphate on the uranium(VI) sorption behavior onto bentonite. *Radiochim Acta* 96:359-366.
- Banning A (2012) Natural arsenic and uranium accumulation and remobilization in different geological environments. Dissertation, RWTH Aachen University.
- Banning A, Demmel T, Rude TR, Wrobel M (2013) Groundwater uranium origin and fate control in a river valley aquifer. *Environ Sci Technol* 47:13941-13948.

- 403 Banning A, Rude TR (2015) Apatite weathering as a geological driver of high uranium con-
404 centrations in groundwater. *Appl Geochem* 59:139-146.
- 405 Blum P, Goldscheider N, Göppert N, Kaufmann-Knoke R, Klinger J, Liesch T, Stober I
406 (2016) Grundwasser - Mensch - Ökosysteme. Karlsruher Institut für Technologie (KIT).
- 407 Breger IA, Deul M (1955) The Organic Geochemistry of Uranium. Contributions to the
408 Geology of Uranium and Thorium by the United States Geological Survey and Atomic
409 Energy Commission for the United Nations International Conference on Peaceful uses of
410 Atomic Energy, Geneva, Switzerland: 505-510.
- 411 Briot P (1983) L'environnement hydrogéochimique du calcrete uranifère de Yeelirrie
412 (Australie Occidentale). *Miner Deposita* 18:191-206.
- 413 Cappuyns V, Swennen R, Nicaes M (2007) Application of the BCR sequential extraction
414 scheme to dredged pond sediments contaminated by Pb-Zn mining: A combined geochemical
415 and mineralogical approach. *J Geochem Explor* 93: 78-90.
- 416 Dahlkamp FJ (1979) Uranlagerstätten. *Gmelin Handbuch der Anorganischen Chemie*.
417 Springer, Heidelberg.
- 418 Deininger RW (1964) Ferrous iron and uranium concentrations and distributions in 100
419 selected limestones and dolomites. Dissertation, Rice University.
- 420 Dickinson M, Scott TB (2010) The application of zero-valent iron nanoparticles for the
421 remediation of a uranium-contaminated waste effluent. *J Hazard Mater* 178(1-3): 171-179.
- 422 Dill HG (1988) Diagenetic and Epigenetic U, Ba, and Base Metal Mineralization in the
423 Arenaceous Upper Triassic "Burgsandstein", Southern Germany. *Miner Petrol* 39(2): 93-105.
- 424 Dill HG (2009) A comparative study of uranium-thorium accumulation at the western edge of
425 the Arabian Peninsula and mineral deposits worldwide. *Arab J Geosci* 4(1): 123-146.
- 426 Dorfner K (1964) Ionenaustauscher. Eigenschaften und Anwendungen. De Gruyter, Berlin.
- 427 Drever HI (1997) The Geochemistry of natural water. Surface and groundwater environments,
428 Prentice Hall, Lebanon.
- 429 Eichfeld S (2004) Methodische und statistische Untersuchungen zur Anwendbarkeit
430 ausgewählter sequentieller Extraktionsverfahren auf bergbautypische Gesteins- und
431 Bodenmaterialien. Dissertation, Friedrich-Schiller-Universität Jena.
- 432 Fernandez HM, Franklin MR, Veiga LHS, Freitas P, Gmiero LA (1996) Management of
433 uranium mill tailing: Geochemical processes and radiological risk assessment. *J Environ*
434 *Radioactiv* 30(1): 69-95.
- 435 Finch R, Murakami T (1999) Systematics and Paragenesis of Uranium Minerals. In: Burns
436 PC, Finch R (Eds.) *Uranium: Mineralogy, Geochemistry and the Environment*: 221-254.
- 437 Füchtbauer H (1988) Sedimente und Sedimentgesteine. Schweizerbart, Stuttgart.

438 Gruner JW (1956) Concentration of uranium in sediments by multiple migration-accretion.
439 Econ Geol 51: 495-520.

440 Heinrichs G, Udluft P (1999) Natural arsenic in Triassic rocks: a source of drinking water
441 contamination in Bavaria, Germany. Hydrogeol J 7: 468-476.

442 Huang PM, Li Y, Summer EM (2011) Handbook of soil sciences. Properties and Processes.
443 Second Edition, CRC, Boca Raton.

444 Jurgens BC, McMahon PB, Chapelle FH, Eberts SM (2009) An Excel Workout for
445 Identifying Redox Processes in Ground Water. U.S. Geological Survey Open-File Report
446 2009-1004.

447 Kelly SD, Newville MG, Cheng L, Kemner KM, Sutton SR, Fenter P, Sturchio NC, Spötl C
448 (2003) Uranyl Incorporation in Natural Calcite. Environ Sci Technol 37: 1284-1287.

449 Kurttio P, Auvinen A, Salonen L, Saha H, Pekkanen J, Makelainen I, Varisanen SB, Penttilla
450 IM, Komulainen H (2002) Renal effects of uranium in drinking water. Environ Health
451 Perspect 110(4): 337-342.

452 Langmuir D (1997) Aqueous Environmental Geochemistry. Prentice Hall, New Jersey.

453 Maia F, Pinto C, Waerenborgh JC, Gonçalves MA, Prazeres C, Carreira O, Sérgio S (2012)
454 Metal partitioning in sediments and mineralogical controls on the acid mine drainage in
455 Ribeira da Água Forte (Aljustrel, Iberian Pyrite Belt, Southern Portugal). Appl Geochem
456 27(6): 1063-1080.

457 Nakata PA (2003) Advances in our understanding of calcium oxalate crystal formation and
458 function in plants. Plant Sci 164: 901-909.

459 Nash JT (1979) Geology, petrology, and chemistry of the Leadville Dolomite: host for
460 uranium at the Pitch Mine, Saguache County, Colorado. U.S. Geological Survey.

461 Nolan J, Weber KA (2015) Natural uranium contamination in major U. S. aquifers linked to
462 nitrate. Environ Sci Technol Letters 2: 215-220.

463 O'Loughlin EJ, Kelly SD, Cook RE, Csencsits R, Kemner KM (2003) Reduction of
464 uranium(VI) by mixed iron(II)/iron(III) hydroxide (green rust): formation of UO₂
465 nanoparticles. Environ Sci Technol 37(4): 721-727.

466 Parkhurst DL, Appelo CAJ (2013) Description of input and examples for PHREEQC version
467 3 – A computer program for speciation, batch-reaction, one-dimensional transport, and
468 inverse geochemical calculations. Denver, Colorado: U.S. Geological Survey, U.S.
469 Department of the Interior, Techniques and Methods, book 6, chapter A43.

470 Radespiel-Tröger M, Meyer M (2013) Association between drinking water uranium content
471 and cancer risk in Bavaria, Germany. Int Arch Occup Environ Health 86: 767-776.

472 Rakovan J, Reeder RJ, Elzinga EJ, Cherniak DJ, Tait CD, Morris DE (2002) Structural
 473 characterization of U(VI) in apatite by X-ray absorption spectroscopy. *Environ Sci Technol*
 474 36: 3114-3117.

475 Regenspurg S, Margot-Roquier C, Harfouche M, Froidevaux P, Steinmann P, Junier P,
 476 Bernier-Latmani R (2010) Speciation of naturally-accumulated uranium in an organic-rich
 477 soil of an alpine region (Switzerland). *Geochim Cosmochim Acta* 74: 2082-2098.

478 Reinhardt L, Ricken W (2000) The stratigraphic and geochemical record of Playa Cycles:
 479 monitoring a Pangaean monsoon-like system (Triassic, Middle Keuper, S. Germany).
 480 *Palaeogeogr Palaeoclimatol* 161: 205-227.

481 Schnug E, Lottermoser BG (2013) Fertilizer-Derived Uranium and its Threat to Human
 482 Health. *Environ Sci Technol* 47(6): 2433-2434.

483 Starinsky A, Katz A, Kolodny Y (1982) The incorporation of uranium into diagenetic
 484 phosphorite. *Geochim Cosmochim Acta* 46: 1365-1374.

485 Sturchio NC, Antonio MR, Soderholm L, Sutton SR, Brannon JC (1998) Tetravalent uranium
 486 in calcite. *Science* 281: 971-973.

487 Tessier A, Campbell PGC, Bisson M (1979) Sequential Extraction Procedure for the
 488 Speciation of Particulate Trace Metals. *Anal Chem* 51(7): 844-851.

489 van Berk W, Fu Y (2017) Redox Roll-Front Mobilization of Geogenic Uranium by Nitrate
 490 Input into Aquifers: Risks for Groundwater Resources. *Environ Sci Technol* 51: 337-345.

491 Wagner SE, Burch JB, Bottai M, Puett R, Porter D, Bolick-Aldrich S, Temples T, Wilkerson
 492 RC, Vena JE, Hébert JR (2011) Groundwater uranium and cancer incidences in South
 493 Carolina. *Cancer Cause Control* 22: 41-50.

494 Welte DH (1962) Sedimentologische Untersuchung uranhaltiger Keupersedimente aus der
 495 Umgebung von Lichtenfels bei Coburg. *Geologica Bavarica* 49: 91-123.

496 Wenzel WW, Kirchbaumer N, Prohaska T, Stingeder G, Lombi E, Adriano DC (2001)
 497 Arsenic fractionation in soils using an improved sequential extraction procedure. *Anal Chim*
 498 *Acta* 436: 309-323.

499 Wrenn ME, Durbin PW, Howard B, Lipsztein J, Rundo J, Still ET, et al. (1985) Metabolism
 500 of ingested U and Ra. *Health Phys* 48(5): 601-633.